X-615-68-232
PREPRINT



# EXPLORER 35 MEASUREMENTS OF LOW ENERGY PLASMA IN LUNAR ORBIT

G. P. SERBU



JUNE 1968

GSFC — GODDARD SPACE FLIGHT CENTER —
GREENBELT, MARYLAND

# EXPLORER 35 MEASUREMENTS OF LOW ENERGY PLASMA IN LUNAR ORBIT

G. P. SERBU
Laboratory for Space Sciences
NASA Goddard Space Flight Center
Greenbelt, Maryland

The purpose of this note is to present some preliminary observations of low energy plasma, E<500eV, taken during lunar orbits of Explorer 35. The spacecraft was injected into a capture lunar orbit on July 22, 1967 at 09:19 U.T. The orbital period is 11.5 hours with an aposelene of 9425 km and a periselene of 2536 km. A good discussion of the transfer trajectory and subsequent lunar orbit has been given by Ness et al (1967).

The plasma measurements reported here were made by means of a planar multi-grid sensor which was programmed as a retarding potential analyzer. The sensor is mounted perpendicular to the spin axis, which is presently oriented within a few degrees of the south ecliptic pole, (R.A. = $99.0^{o}$ DEC. = $-67.5^{o}$). The magnitude and polarity of the plasma current at the sensor is measured as a function of retarding potential in the interval from -500 to +500 volts. For example, the retarding potential analyzer effectively separates out from the entering plasma those ions with energies below 15 eV, and measures the net negative current as a function of retarding potential in the interval from +6 to -15 volts. The measurements are then extended to energies up to 500 eV, and they are repeated for opposite polarities; in this manner the integral spectrum for both electrons and ions is obtained in the energy range from 0 to 500 eV.

The collector current is measured by a logarithmic electrometer which is sensitive to both current polarities in the range from $1x10^{-6}$ to $3x10^{-12}$ amperes. The electrometer output is digitized into a seven bit word and then presented to telemetry. After the 8th lunar orbit of July 25, 1967 a malfunction occurred in the digitizing circuit and no additional data was recovered from this experiment until January 12, 1968. On this date the experiment again returned to normal operation, and good quality information has been obtained continuously since that time. The experiment is calibrated internally once every 5 minutes, consequently a high degree of confidence is placed on the measured values obtained.

Some preliminary observations based on the measured electron integral currents in the retardation interval from -15 to +6 volts are presented at this time. Two electron current-voltage characteristics are shown in Figure 1. During the time interval of these observations the satellite traversed the altitude range from 1050 km to 1920 km above the lunar surface and it entered the optical shadow of the moon at 19:55 UT. The top curve of Figure 1 is an electron current-voltage characteristic which was obtained 4 minutes before shadow entry and it is representative of electron measurements obtained in the solar wind region, with the satellite in sunlight. The circle and triangle data points plot the measured value of negative current for each retarding voltage. The gaps in the data near -8 and 0 volts are due to discarded measurements. These measurements are not plotted because they contain spurious photo-electron currents from within the sensor, which are observed when the sensor normal is oriented within $\pm 85^{o}$ of the sun vector. A two-component Maxwellian distribution is observed in the electron spectrum obtained in

sunlight. The slopes of the two components have been indicated in the figure with light lines. The dashed-curve drawn through the data points indicates that toward increasing electron retardation, the electron current has an exponential dependence of the type $I=I_o e^{-eV/kT}$. Where eV is the energy of the electrons, k is Boltzmann's constant, T is the temperature and $I_o$ is the current measured at the spacecraft potential. The energetic component of the measured spectrum, is ascribed as due to the solar wind electrons, at a temperature of $7.4 \times 10^4$ $^oK$ and a density of 8 electrons $cm^{-3}$. When the solar wind component is subtracted from the plotted data, a second component is evident with a peak current value of $2 \times 10^{-9}$ amperes and a temperature of $1.4 \times 10^4$ $^oK$. This secondary, or low energy, component observed when the spacecraft is in sunlight is interpreted in terms of a photo-electron cloud which envelops the spacecraft as a consequence of solar illumination. This type of spacecraft=associated photo-electron cloud was first described by Wolfe et al (1967) in connection with observations on Pioneer VI.

The squares in Figure 1 represent a plot of the electron data obtained 18 minutes after the spacecraft entered the optical shadow of the moon; note that no data gaps exist when the measurement is made in the absence of solar ultraviolet illumination. A similarity between the electron spectrum in sunlight and shadow is evident, with the current magnitude of the shadow curve being depressed by about a factor of 10. Currents below $1 \times 10^{-11}$ amperes are within the noise level of the instrument, therefore, no definite assurance exists as to the true shape of the curve in lunar shadow at retardation

greater than -3 volts. The observed electron current, with the spacecraft in shadow, also indicates the presence of a low energy ($10^4$ $^oK$) component. A similar low energy electron current was observed in the lunar shadow with the charged particle traps onboard LUNA 10. Gringauz et al (1967) tentatively identified this current as due to a lunar ionosphere, at an altitude 300-1000 km above the moon, with a density value of between 15 to 20 electrons/$cm^{-3}$ at a temperature of about $10^4$ $^oK$.

Ion currents due to such a tenuous lunar ionosphere would be barely observable in our experiment. The electron data of Figure 2, however, shows that the magnitude of the electron current measured at the satellite potential is a function of position within the shadow; minimum currents are observed at the core of the umbra and not at the maximum height above the lunar surface as would be expected for a lunar ionosphere. The possibility does exist that the low energy component, observed in the lunar shadow is a measure of secondary electrons emitted from the satellite surface as a consequence of bombardment by a high energy electron flux, E<30KeV, such as observed on LUNA 11 by Grigorov et al (1967).

Presented in Figure 2 are a series of spectrums which illustrate the type of data obtained through the lunar shadow with the retarding potential analyser. At the top of the figure is shown the pertinent portion of the orbital pass of January 29, 1968, through the lunar shadow as seen projected onto the ecliptic plane. On the 29th the moon was located in the undisturbed solar wind region. The numbered tick marks

along the orbital path refer to the sequential time order in which the labelled electron spectrums, plotted in the lower portion of Figure 2, were obtained. The time of observation is given in the legend. The 55 minute orbital pass through the shadow occurred some 20 minutes after perigee at a distance of from 1.8 to 3.0 lunar radii behind the moon. At perigee the satellite orbital velocity is 1.74 km/sec, it decreases to 1.25 km/sec one hour past perigee; therefore, for all orbital positions the satellite velocity is low even when compared to a thermal proton ($10^4$ $^oK$) which has a velocity of 13 km/sec. Throughout the entire orbit, therefore, the satellite motion through the plasma can be ignored, and the collected currents can be considered in terms of Langmuir theory.

Due to data drop-out, the current-voltage characteristics of Figure 2 labelled 1 and 2 were not carried to saturation. A measure of the solar wind electron temperature can be made on the basis of the data to the left of zero volts retardation from the characteristics labelled 1, 2 and 5. The temperature obtained from the slope of these curves is $8.4 \times 10^4$ $^oK$, in agreement with the measurement obtained at location S, which occurs just subsequent to emergence from shadow. These observations indicate that no appreciable cooling of the electron plasma occurs as a consequence of expansion into the void.

Providing that the electron temperature remains constant in the plasma void; the variation in the magnitude of the measured current at a fixed voltage on the characteristic may be used to deduce the relative variation of the electron

density throughout the plasma void. The voltage point on the characteristic is chosen to be within a fraction of a kT from the satellite potential, and yet sufficiently retarding so that low energy currents are negligible. The zero volt point on the characteristics of Figure 2 fits the above selection process and was used to drive a ratio of shadow-to-sunlight current as a function of orbital position. This ratio was then normalized to the density value measured in sunlight.

Using the above criterion, the observed density ratio at location 1 is 0.07, when taken with respect to the measurement at location S, where the spacecraft is in sunlight. At location 2 the ratio is down to 0.03 and still decreasing toward the minimum of less than 0.01 observed at locations 3 and 4. The minimum ratio is observed almost coincident with the geometric core of the umbra, this type of coincidence between plasma minimum and umbra core is generally, but not always, observed. At location 5, the ratio is 0.03 and it increases to 1.0 when the spacecraft is in sunlight at location S. This type of density decrease toward a minimum with a subsequent recovery is evident in the measurement whenever the lunar shadow is traversed.

A variation in the spacecraft-to-plasma potential as a function of orbital position through the shadow is also evident in Figure 2. The potential changes from -5 volts at the core of the umbra to -3.9 volts at location 5; and in sunlight, the potential is -1.5 volts.

Thus, a clear identification of spacecraft potential change is evident in the figure. The observed spacecraft-to-plasma potential shift from -1.5 volts in sunlight to -5 volts in core of the lunar shadow, is consistent with the expectation that solar illumination will drive a satellite to a more positive potential as a consequence of photo-electron emission from the surface.

Some additional data obtained in the plasma void are presented in Table 1. Measured values of satellite potential and electron temperature, along with the computed density ratio $N/N_o$, are tabulated as a function of the seleneocentric solar ecliptic coordinates ($X_{SSE}$, $Y_{SSE}$) in lunar radii. Values for three crossings made in the solar wind region, and one in the Earth's extended magnetosheath region are tabulated. Apparent for all crossings is a very steep gradient in the computed plasma density ratio, $N/N_o$, which is observed on the inside surface of the optical shadow. Generally, the plasma density falls below 10% of the value measured in sunlight within the first ten minutes after entry into the shadow region. Insufficient spatial resolution precludes the detection of any misalignment between the optical shadow boundary and the boundary of the plasma void, such a misalignment would be a function of the upstream solar wind flow direction.

The transit of March 4 closely matches the transit discussed by Michel (1968). Along this orbital path, i.e. within 1.5 lunar radii behind the moon, he predicts that the density will fall to 10% of the ambient within 15 minutes after entry into the plasma void. January 19 is of interest since it is to date the crossing at the greatest distance behind the moon

observed with this experiment. No clear shock crossing indication is evident in this data, which was obtained at 3.18 $R_m$ behind the moon. Behind the standing shock, the plasma void should disappear; however, as Michel (1967) points out, the geometry, location and intensity of the shock are highly variable in terms of upstream plasma and field conditions, more extensive observations are clearly needed. The kinetic theory approach of Whang (1968) predicts that the plasma void extends tens of lunar radii behind the moon, without the formation of a standing shock. Ness et al (1968) support this prediction with the observation that no standing shock has been detected in the magnetic field downstream of the moon.

## Conclusions

Some descriptive characteristics of the lunar void, based on recent observations obtained from the Explorer 35 integral electron spectrums, are: (1) the electron density within the lunar plasma void is generally less than 10% of the observed density in sunlight. A very steep density gradient is observed upon entry and exit from the plasma void. (2) The lunar plasma void has been detected to be nearly coincident with the optical shadow to distances of 3.18 lunar radii behind the moon. (3) No measurable cooling of the electrons is noted within the plasma void.

Although a detailed analysis of the data has not been completed, it is tentatively concluded that no clear evidence exists for a lunar ionosphere at altitudes in excess of 825 km above the surface. Our results also show that a characteristic variation in satellite-to-plasma potential is observed as a direct consequence of solar illumination.

## FIGURE TITLES

Figure 1 - Electron current-voltage characteristics obtained in lunar orbit with the Explorer 35 Retarding Potential Analyzer experiment. These observations illustrate the variations in current magnitude, and changes in satellite potential, $V\phi$, as the spacecraft moves from sunlight into the lunar shadow.

Figure 2 - A series of sequential time observations of a systematic variation in the measured electron currents as a function of orbital position through the lunar shadow.

Table 1 - Observations of the lunar plasma void, deduced from the observed gradient in the electron plasma density ratio and changes in the spacecraft-to-plasma potential.

## REFERENCES

Grigorov, N. L., V. I. Lutsenko, V. L. Maduyev, N. F. Pisarenko, I. A. Savenko, Registration of Electrons with Energies <30 KeV in the near-Lunar Space, Kosmicheskiye Issledovaniya Tom 5, Vypusk 6, Str. 891-896, Izdatel'stvd "Nauka", 1967.

Gringauz, K. I., V. V. Bezrukikh, M. A. Khokhlov, G. N. Zastenker, A. P. Remizov, L. S. Musatov, Results of Experiments for the Detection of Lunar Ionospheres carried out on the first Moon's artificial satellite (LUNA-10), Doklady A. N. SSR, Geofizika Tom 170, No. 6, pp 1306-1309, Izdatel'stvo "Nauka", 1966.

Michel, F. C., Shock Wave Trailing the Moon, J. Geophys, Res., 72, 5508-5509, 1967.

Michel, F. C., Magnetic Field Structure behind the Moon, J. Geophys. Res., 73, 1533-1542, 1968.

Ness, N. F., K. W. Behannon, C. S. Scearce, and S. C. Cantarano, Early Results from the Magnetic Field Experiment on Lunar Explorer 35, J. Geophys. Res., 72, 5769-5778, 1967.

Ness, N. F., K. W. Behannon, H. E. Taylor, Y. C. Whang, Perturbations of the Interplanetary Magnetic Field by the Lunar Wake, to be published in the J. Geophys. Res., GSFC Document X-612-68-12, 1968.

Whang, Y. C., Interaction of the Magnetized Solar Wind with the Moon, NASA-GSFC Preprint X-612-67-580, 1967.

Wolfe, J. H., R. W. Silva, D. D. McKibbin, The Interplanetary Solar Wind Electron Characteristics, Trans. Amer. Geophys. Union 48, 182, 1967.

# EXPLORER - 35 JANUARY 28, 1968

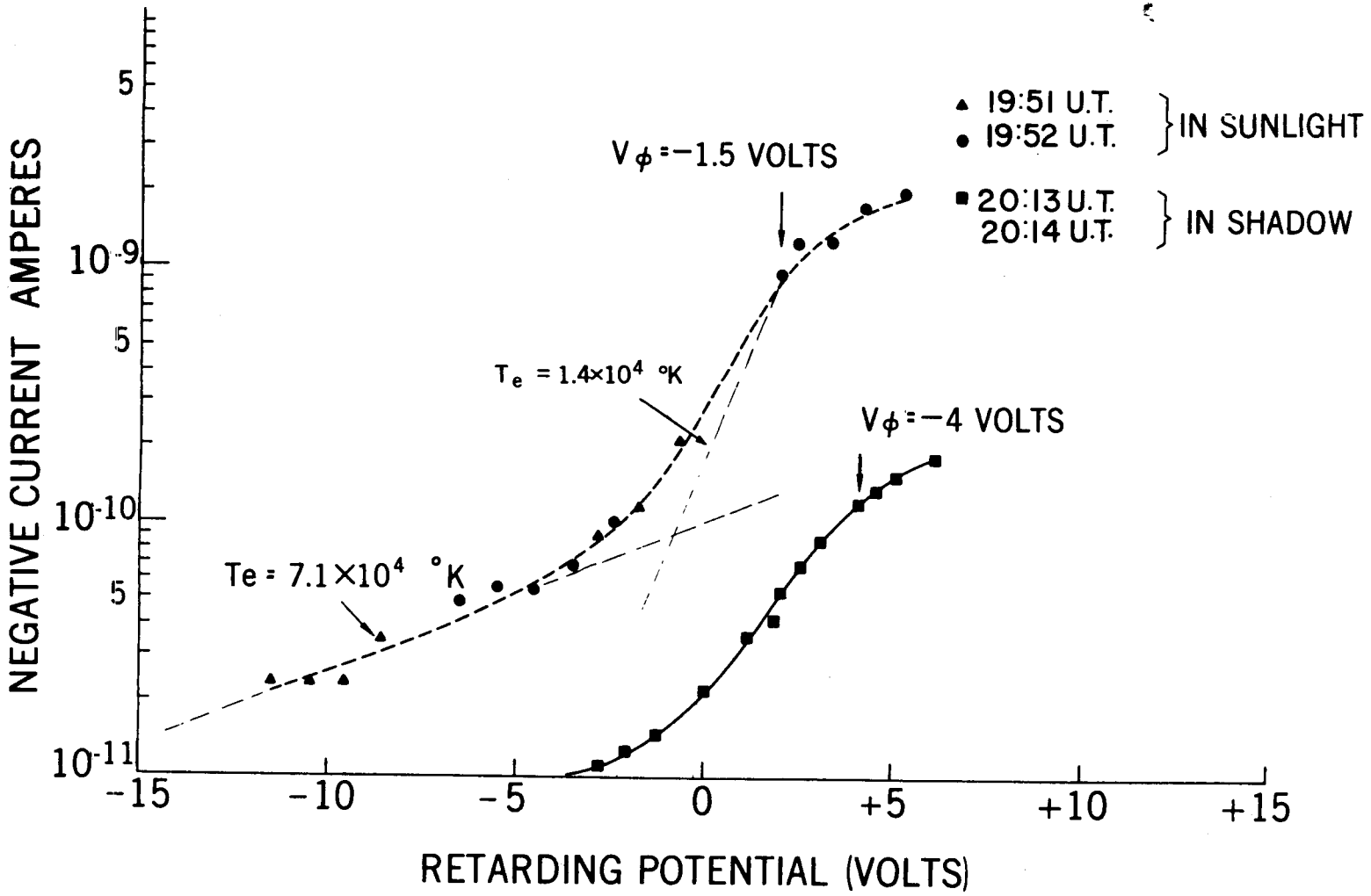

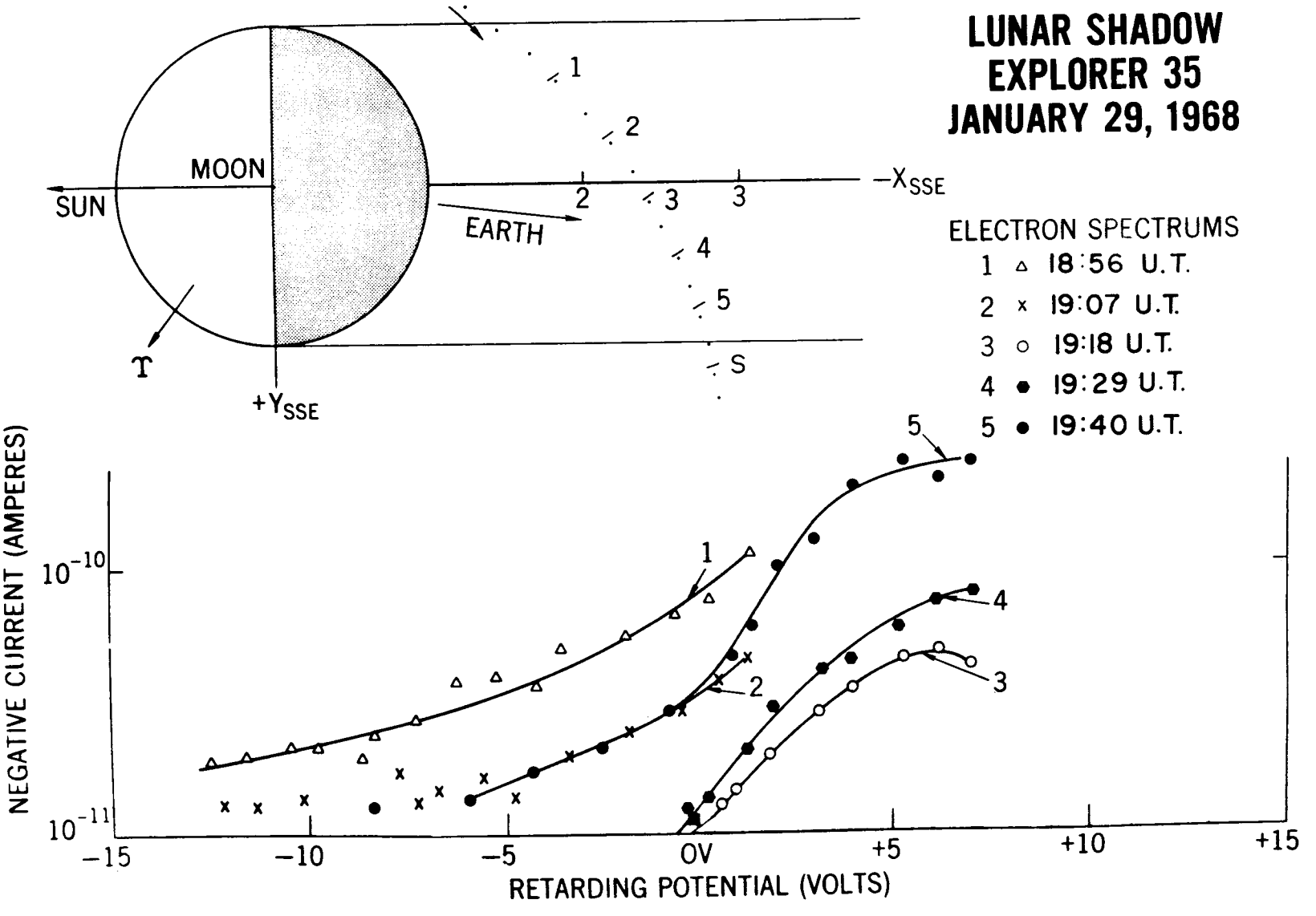
LUNAR SHADOW
EXPLORER 35
JANUARY 29, 1968
MOON
SUN
EARTH
$-X_{SSE}$
$+Y_{SSE}$
ELECTRON SPECTRUMS
1 △ 18:56 U.T.
2 × 19:07 U.T.
3 ○ 19:18 U.T.
4 ● 19:29 U.T.
5 ● 19:40 U.T.
NEGATIVE CURRENT (AMPERES)
$10^{-10}$
$10^{-11}$
−15
−10
−5
0V
+5
+10
+15
RETARDING POTENTIAL (VOLTS)

# TABLE 1

| DATE | TIME | S/C POTENTIAL VOLTS | $T_e$ (°K) | N/No | COORDINATES ($F_M$) $X_{SSE}$ | $Y_{SSE}$ | REGION |
|---|---|---|---|---|---|---|---|
| JAN. 19, 1968 | 19:10 | −2.0 | $6.2 \times 10^4$ | 1.00 | −3.40 | +2.12 | |
| | 19:32 | −3.1 | | .14 | −3.05 | +0.66 | MAGNETO-SHEATH |
| | 19:40 | −3.1 | | .16 | −3.14 | +0.98 | |
| | 19:44 | −3.0 | | .20 | −3.18 | +1.04 | |
| JAN 28, 1968 | 19:41 | −1.2 | $7.1 \times 10^4$ | 1.00 | −0.94 | −1.20 | |
| | 19:52 | −1.4 | | .43 | −1.44 | −1.00 | |
| | 20:03 | −2.7 | | .26 | −1.82 | −0.64 | SOLAR WIND |
| | 20:15 | −4.0 | | .24 | −2.14 | −0.28 | |
| | 20:26 | −1.5 | | .57 | −2.40 | +0.14 | |
| JAN. 29, 1968 | 18:57 | −3.2 | | .07 | −1.86 | −0.62 | |
| | 19:08 | −3.2 | | .03 | −2.18 | −0.25 | |
| | 19:19 | −5.0 | | .01 | −2.44 | +0.10 | SOLAR WIND |
| | 19:30 | −4.8 | | .01 | −2.61 | +0.48 | |
| | 19:41 | −3.9 | | .03 | −2.76 | +0.80 | |
| | 19:53 | −1.5 | $9.4 \times 10^4$ | 1.00 | −2.84 | +1.14 | |
| MARCH 4, 1968 | 20:29 | −2.5 | $1.2 \times 10^5$ | 1.00 | −1.00 | −1.10 | |
| | 20:40 | −5.6 | | .02 | −1.55 | −0.60 | |
| | 20:51 | −5.6 | | $< .01$ | −1.85 | −0.10 | SOLAR WIND |
| | 21:02 | −4.3 | | $< .01$ | −1.95 | +0.45 | |
| | 21:12 | −3.4 | $1.2 \times 10^5$ | 1.00 | −2.00 | +1.05 | |